New Physics: Sae Mulli,
Vol. 69, No. 12, December 2019, pp. 1299∼1302
http://dx.doi.org/10.3938/NPSM.69.1299

LCD Glass Defect Inspection Using a Digital Holographic Microscope

Sanghoon SHIN
Kanghae Precision System, Hwaseong 18487, Korea

Younghun YU*
Department of Physics and Research Institute for Basic Sciences, Jeju National University, Jeju 63243, Korea

(Received 02 September 2019 : revised 30 October 2019 : accepted 04 November 2019)

Quality control of glass for display is a crucial issue, and defects existing in glass can dramatically degrade the quality of display devices. In optical path system, these defects cause different degrees of scattering to the beam, destroy the uniformity of the light field and reduce the beam quality. Here, we present the use of a digital holographic microscope as a tool for inspecting two- and three-dimensional defects. Glass quality control is an important issue in the manufacture of displays, and display quality can be degraded significantly by the presence of defects. We have demonstrated that defects can be quickly inspected and characterized through use of a digital holographic microscope, and we verified the results by comparing the images obtained using the digital microscope to the those captured using a through comparison to images captured using a confocal microscope.

PACS numbers: 42.40.Kw, 42.40.−i, 07. 60. Pb
Keywords: Digital holography, Off-axis holography, Defect inspection

I. INTRODUCTION

In recent years, the rapid development of information technology has led to an era in which data can be accessed anytime and anywhere; the importance of the display technologies used to visualize this information has increased accordingly.

The appearance and function of liquid crystal displays (LCDs) are, in part, dependent on the surface quality of the end-product. Transparent surfaces, such as covering glass, touch panels, and LCDs, are sensitive to defects, which can disrupt the uniformity of the light field and reduce the beam quality of optical systems [1,2]. Owing to imperfections in processing and operating environments, most optical components exhibit surface defects such as scratches and pitting. Therefore, numerous techniques have been developed to quantify defect structures on the surface of optical elements [3–7]. Surface defects found on optical elements are typically small, sparsely distributed, and fragile; therefore, high-resolution, efficient and non-destructive detection techniques must be employed. Defect shapes can be measured in two dimensions (2-D) using dark-field imaging. However, the three-dimensional (3-D) structure of the defect cannot be fully determined, so it is difficult to accurately analyze the effect that defects differing in shape and size have on the optical field [8,9].

Presently, confocal microscopes (CMs) are used for both 2-D and 3-D defect measurements. The resolution and image quality are sufficient for defect characterization, but measurements are time-consuming [10]. Recently, digital holography (DH) has been employed for 3-D measurements using a 2-D digital camera, in which amplitude and phase changes attributable to diffraction by an object are recorded simultaneously [11–14]. DH has received increased attention owing to its ease of use and potential for quantitative phase imaging. DH is used in a wide range of fields, such as fluid mechanics [15, 16], biomedical imaging [17,18], and mechanical vibration analysis [19,20]. The availability of high-resolution

*E-mail: yyhyoung@jejunu.ac.kr

charge-coupled devices (CCD) and complementary metal oxide semiconductor (CMOS) sensors contributed to the development of digital reconstruction techniques. Specifically, DH was made feasible by recent advances in megapixel CCD and CMOS sensors with high spatial resolution.

In this paper, we propose a fast and nondestructive microscopic glass defect observation method based on DH technology, in which defect morphology is obtained by phase calculation; the performance is compared to that of CM images.

II. THEORETICAL MODEL

During the hologram-recording process, a plane reference wave, R, and object wave, O, interfere at the CCD or CMOS. The hologram intensity is given by

$$I_H(x,y) = |R|^2 + |O|^2 + R^*O + RO^* \tag{1}$$

where $|R|^2$ and $|O|^2$ are the intensities of the reference wave and object wave, respectively. R^*O and RO^* represent the interference terms, where R^* and O^* denote the complex conjugates of the two waves [11–14].

Mathematically, the amplitude and phase distributions in the real image plan can be calculated by applying the Fresnel–Kirchhoff integral to a filtered hologram. If a plane wave illuminates the hologram with an amplitude transmittance of $I_H(x,y)$, the Fresnel-Kirchhoff integral yields a complex amplitude $\Psi(\xi,\eta)$ in the real image plane, as

$$\Psi(\xi,\eta) = \frac{\exp\left(\frac{i2\pi d}{\lambda}\right)}{i\lambda d}\exp\left[\frac{i\pi}{d\lambda}(\xi^2+\eta^2\right] \times \int\int I_H(x,y)\exp\left[\frac{i\pi}{d\lambda}(x^2+y^2\right]\exp\left[\frac{i2\pi}{d\lambda}(\xi x+\eta y)\right]dxdy \tag{2}$$

where λ is the wavelength and d is the reconstruction distance. (x,y) is the spatial coordinate in hologram plan. From Eq. (3), the Fresnel-Kirchhoff integral can be considered as the Fourier transformation of the function $I_H(x,y)\exp[i\pi(x^2+y^2)/d\lambda]$ at spatial frequencies ξ and η. Because $\Psi(\xi,\eta)$ is an array of complex numbers, an amplitude image can be obtained using the intensity [11–14]:

$$I(\xi,\eta) = \mathrm{Re}[\Psi(\xi,\eta)]^2 + \mathrm{Im}[\Psi(\xi,\eta)]^2 \tag{3}$$

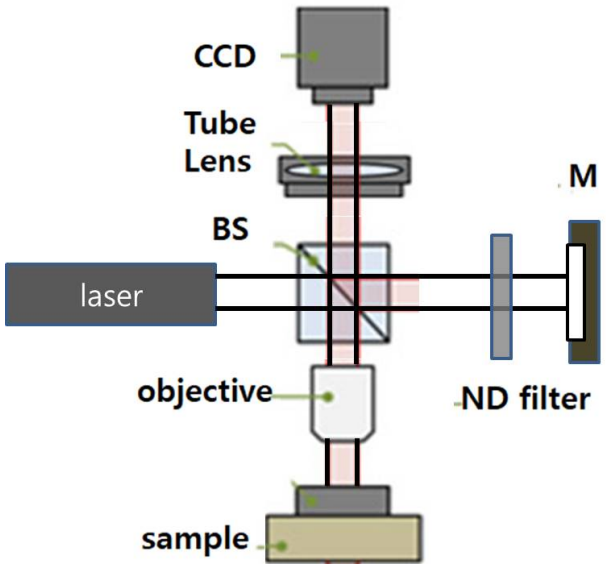

Fig. 1. (Color online) Schematic diagram of the experimental apparatus, showing the beam splitter (BS), mirror (M), charge-coupled device (CCD), and neutral-density filter (ND).

The quantitative phase image is obtained by calculating the argument

$$\phi(\xi,\eta) = \arctan\left[\frac{\mathrm{Re}[\Psi(\xi,\eta)]}{\mathrm{Im}[\Psi(\xi,\eta)]}\right] \tag{4}$$

The real 3-D information is acquired by phase unwrapping of the quantitative phase image according to Eq. (4) [21].

III. Experiment and Results

Figure 1 shows a schematic diagram of the off-axis reflective-type digital holographic microscope. The experimental set up is comparable to that of a Mach-Zender interferometer. A 632-nm He:Ne laser was used as the light source, and the holograms were recorded using a CCD camera (Imperx). Images comprised 1,024 × 1,024 pixels, and each pixel measured 7.4 μm × 7.4 μm. The angle between the reference and object beams was approximately 2°, which resulted in separation (according to Eq. (1)) in the 2-D spatial frequency domain. Real and twin images of the object were created as described in Eq. (1). Filtering in the spatial frequency space was used to improve the quality of the image reconstruction by discarding the DC and twin image terms [14].

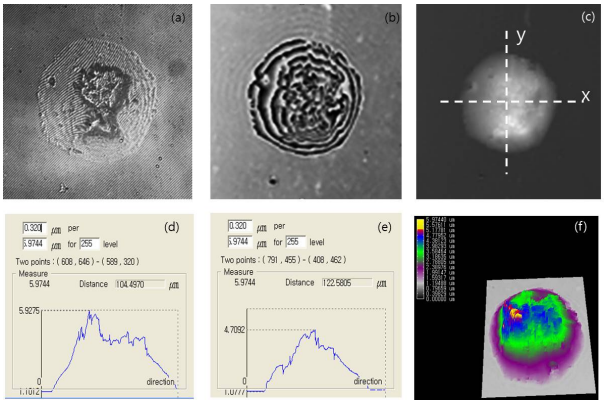

Fig. 2. (Color online) Holographic and reconstructed images of a defect, specifically the (a) hologram, (b) wrapped and (c) unwrapped quantitative phase images, (d) x and (e) y profiles of the dashed lines in (c), and a (f) three-dimensional (3-D) image of the defect.

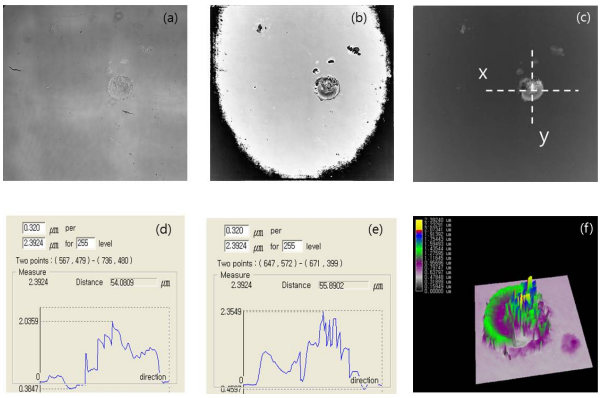

Fig. 3. (Color online) Hologram and reconstructed images of a defect, showing the (a) hologram, (b) wrapped and (c) unwrapped quantitative phase images, (d) x and (e) y profiles of the dashed lines in (c), and a (f) 3-D image of the defect.

Figure 2 shows the measurement of a glass surface defect. Figures 2(a) and (b) show the hologram and reconstructed wrapped quantitative phase image, respectively. The wrapped quantitative phase image was calculated using Eq. (2), Eq. (4), and the filtered hologram. Flynn' s minimum discontinuity phase unwrapping method [20] was used to produce the unwrapped real phase image in Figure 2(c). Figures 2(d) and (e) show the profiles along the dashed x and y lines in Figure 2(c), respectively, and Figure 2(f) shows the 3-D structure of the defect.

Figure 3 shows the experimental results of a glass surface defect of another sample.

Figures 3 (a), (b) and (c) show the hologram, and wrapped and unwrapped quantitative phase images, respectively. Figures 3 (d) and (e) are the x and y profiles along the dashed lines shown in Fig. 3(c) and Fig. 3 (f) illustrates the 3-D structure of the defect.

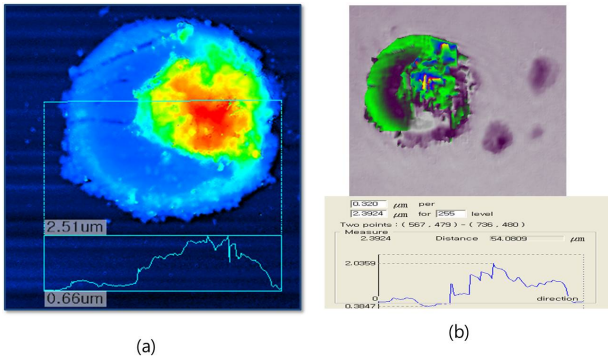

Fig. 4. (Color online) Comparison of the (a) confocal microscope and (b) digital holographic microscope images and profiles.

The images captured using the digital holographic microscope were verified by comparison to the images from a CM, as shown in Fig. 4(b) and Fig. 3 (c) are equivalent.

Figure 4(a) shows the unwrapped quantitative phase image and profile taken with the CM; those captured using the digital holographic microscope (DHM) are shown in Figure 4(b). The measurement times of the CM and DHM were 150 s and 2 s respectively; thus, capturing images with the DHM is faster than with the CM. It can also be seen that the quantitative phase images and profiles of the two images are similar. From Figure 4, we can conclude that DHM could be used to quickly identify defect structures in glass surfaces.

IV. Conclusion

We have demonstrated the use of a digital holographic microscope for 2-D and 3-D defect inspection. Common optical element surface defects are small, sparsely distributed, and fragile; therefore, the detection method needed to be high-resolution, efficient, and non-destructive. Through comparison to images captured using a CM, we have verified that defects can be quickly characterized and inspected using a digital holographic microscope. Here, we have shown that digital holographic microscopy could be used for inspecting glass surfaces, and verifying defect structures.

REFERENCES

[1] J. Fournier *et al.*, Opt. Mater. Express **3**, 1 (2013).

[2] S. Demos, M. Staggs, K. Minoshima and J. Fujimoto, Opt. Express **10**, 1444 (2002).

[3] M. K. Dai and X. D. Yan, Optical Instruments **18**, 33 (1996).

[4] X. Peng, *et al.*, Int. J. Adv. Manuf. Technol. **39**, 1180 (2008).

[5] E. Laizola *et al.*, SPIE **5011**, 90 (2003).

[6] Y. Zhang, W. Jing, H. Zhang and L. Haifeng, Opt. Precision Eng. **12**, 560 (2004)

[7] F. Wang, Y. Yang, D. Sun, L. Yang and R. Li, Proc. SPIE **6150**, 61500F-1 (2006).

[8] K. C. Fan, S. H. Chen, J. Y. Chen, and W. B. Liao, NDT & International **43**, 451 (2010).

[9] K. C. Fan, L. Y. Chen, X. Yu and L. Yan, Proc. SPIE **10818**. 108181J (2018).

[10] B. Rappaz *et al.*, Cytometry A **7**, 895 (2008).

[11] L. P. Yaroslvsky, *Methods of digital holography* (Consultant Bureau, New York, 1980).

[12] L. Onural and P. D. Scott, Opt. Eng. **26**, 1124 (1987).

[13] U. Schnars and W. Jüptner, Appl. Opt. **33**, 179 (1994).

[14] E. Cuche, P. Marquet and C. Depeursinge, Appl. Opt. **39**, 4070 (2000).

[15] H. Meng, G. Pan, Y. Pu and S.H.Woodward, Meas. Sci. Technol. **15**, 673 (2004).

[16] N. Verrier *et al.*, Opt. Express **18**, 7807 (2010).

[17] F. Charrière *et al.*, Opt. Express **14**, 7005 (2006).

[18] M.K. Kim, Opt. Express **7**, 305 (2000).

[19] A. Asundi and V.R. Singh, Appl. Opt. **45**, 2391 (2006).

[20] F. Joud *et al.*, Opt. Express **17**, 2774 (2009).

[21] D. C. Ghiglia and M. D. Pritt, *Two-Dimensional Phase Unwrapping* (John Wiley & Sons, New York, USA, 1998).